

## Hematopoietic stem cells debut in embryonic lymphomyeloid tissues of elasmobranchs

Rosa Manca,<sup>1</sup> Chester A. Glomski,<sup>2</sup>  
Alessandra Pica<sup>1</sup>

<sup>1</sup>Department of Biology, University of  
Naples Federico II, Italy

<sup>2</sup>Department of Pathology and  
Anatomical Sciences, Jacobs School of  
Medicine, State University of New York,  
Buffalo, NY, USA

### Abstract

The evolutionary initiation of the appearance in lymphomyeloid tissue of the hemopoietic stem cell in the most basal vertebrates model, *i.e.* the elasmobranch (chondrichthyan) *Torpedo marmorata* Risso, has been studied. The three consecutive developmental stages of torpedo embryos were obtained by cesarean section from a total of six pregnant torpedoes. Lymphomyeloid tissue was identified in the Leydig organ and epigonal tissue. The sections were treated with monoclonal anti-CD34 and anti-CD38 antibodies to detect hematopoietic stem cells. At stage I (2-cm-long embryos with external gills) and at stage II (3-4 cm-long embryos with a discoidal shape and internal gills), some lymphoid-like cells that do not demonstrate any immunolabeling for these antibodies are present. Neither CD34+ nor CD38+ cells are identifiable in lymphomyeloid tissue of stage I and stage II embryos, while a CD34+CD38- cell was identified in the external yolk sac of stage II embryo. The stage III (10-11-cm-long embryos), the lymphomyeloid tissue contained four cell populations, respectively CD34+CD38-, CD34+CD38+, CD34-CD38+, and CD34-CD38- cells. The spleen and lymphomyeloid tissue are the principal sites for the development of hematopoietic progenitors in embryonic *Torpedo marmorata* Risso. The results demonstrated that the CD34 expression on hematopoietic progenitor cells and its extraembryonic origin is conserved throughout the vertebrate evolutionary scale.

### Introduction

Embryonic hematopoiesis has been extensively studied in mammalian species, while this process remains incompletely explored in the most basal vertebrates. The developmental changes that have transpired

in vertebrates during evolution concerning the debut of the hematopoietic stem cell (HSC) and the selection of the sites of hemopoiesis await investigation.

HSCs require a specific microenvironment, the hematopoietic niche, for cell homeostasis. Hematopoietic sites change during vertebrate ontogeny and the factors that regulate homing to hematopoietic sites have not been identified. It is known that in most vertebrates, HSCs derive from an extra-embryonic location in the yolk sac and later migrate within the organism to form the primitive and definitive hematopoietic lineages.<sup>1</sup>

In mammalian embryos, specifically, hematopoietic cells are observed to originate in the extra-embryonic yolk sac and the intraembryonic para-aortic splanchnopleura/aorta-gonad-mesonephros region (AGM).<sup>2</sup> Tavian *et al.*<sup>3,4</sup> demonstrated that the intra-aortic hematopoietic clusters (IAHCs) cover the preumbilical area of the floor of the dorsal aorta and penetrate the vitelline artery; at 19 days post-conception, the human dorsal aorta endothelial cells upregulate CD34 and the first CD34+CD45+ cells emerge in the pre-umbilical region of the dorsal aorta (33 days post conception).

At 5-6<sup>th</sup> week of development, the human placenta contains high numbers of CD34+CD38- cells and contains numerous colony forming units-culture (CFU-C). In the mammalian vertebrate embryo, the hematopoietic cells, from yolk sac and AGM region, sequentially migrate to the liver (midgestational stages) and to the bone marrow (neonatal stages) to create the adult hematopoietic system.<sup>5,6</sup> However, this sequential migration has not been directly demonstrated in mammalian species,<sup>7</sup> while Medvinsky and Dzierzak<sup>8</sup> have demonstrated that the AGM region is the source of the definitive adult hematopoietic system, which subsequently colonizes the liver.

Among most basal vertebrates, such as, aquatic vertebrates, in teleosts, such as the angelfish, killifish, and zebrafish, the embryonic blood cells originate in the yolk sac and in the intercellular mass confined within the distinct dorsal-lateral compartment.<sup>1,9</sup> In zebrafish, embryonic hematopoiesis is a multistep process, occurring in three distinct waves. During the primitive wave, the medial and anterior lateral mesoderm give rise to embryonic erythroid and myeloid cells, respectively. Erythro-myeloid progenitors form in the posterior blood island (PBI) during a transient intermediate wave. Finally, during the definitive wave, hematopoietic stem cells originate in the AGM. The HSCs then translocate to and expand in the caudal hematopoietic tissue, which is followed by

Correspondence: Alessandra Pica, Department of Biology, University of Naples Federico II, Via Cinthia 26, 80126 Napoli, Italy.  
Tel. +39.081.2535054/040.  
E-mail: alessandra.pica@unina.it

Key words: Hematopoietic stem cells; embryonic hemopoiesis; CD34+/CD38- cells; progenitor cells; elasmobranchs; torpedoes.

Contributions: AP, CAG, conceived the ideas and the study; AP, CAG, RM, designed the research, analyzed the data and wrote the manuscript; AP, performed most experiments (double immunocytochemistry and histology). All authors discussed the results and commented on the manuscript.

Received for publication: 18 July 2019.

Accepted for publication: 21 September 2019.

This work is licensed under a Creative Commons Attribution-NonCommercial 4.0 International License (CC BY-NC 4.0).

©Copyright: the Author(s), 2019

Licensee PAGEPress, Italy

European Journal of Histochemistry 2019; 63:3060  
doi:10.4081/ejh.2019.3060

the colonization of the kidney and the thymus. Interestingly, it was recently discovered that HSC independent T-cells can originate from the AGM and PBI during the embryonic and larval stages of development.<sup>10,11</sup>

In adult teleosts, hematopoiesis occurs in the kidney which can be considered analogous to the mammalian bone marrow.<sup>12</sup>

On the other hand the embryonic origin of HSC in cartilaginous fishes is not fully documented. While the adult hemopoiesis of cartilaginous fishes has been described by Pica and Della Corte<sup>13</sup> and by Medvinsky and Dzierzak<sup>8</sup>, no studies concerning the embryonic origination of the HSC have been conducted in elasmobranchs.

The lymphomyeloid system plays a fundamental role in hematopoiesis and in the immune response of elasmobranchs. It consists of mixed lymphoid and myeloid elements and are less specialised in structure and function than the corresponding mammalian tissue. However the cells identified in the lymphomyeloid system of the shark *Etmopterus spinax* have cytological features similar to mammalian cells.<sup>14</sup> The elasmobranch lymphomyeloid system represents 0.5-1.5% of total body weight. The cellular composition of lymphohemopoietic tissue in the wall of the esophagus, termed the Leydig organ, and epigonal tissues are remarkably similar, both containing large numbers of developing granulocytes, blast cells, lymphocytes, and plasma cells. The

mature cells can migrate through the walls of sinusoidal blood vessels. The structure and ultrastructure of elasmobranch's leukocytes have been described by Pica *et al.*<sup>15</sup> and Fänge.<sup>16</sup>

The lymphomyeloid Leydig organ is first found at the external gill embryonic stage and becomes more prominent during the interval of the sixth to the eighth month. Immature granulocytes and lymphocytes have been detected by the electron microscopy.<sup>16</sup>

Lloyd-Evans<sup>17</sup> studied the Leydig and the epigonal organ development in the chondrichthyan *Scyliorhinus canicula*. Its esophageal lymphomyeloid Leydig organ consists leukocytes of that are tightly packed and arranged into dorso-ventral strands, that are separated by blood sinuses.

The Leydig organ is detectable in the 2 cm-long embryo of *Torpedo marmorata* and in the 3.5 cm-long dogfish embryo *Scyliorhinus canicula*. Granulopoietic cells appear in the parenchyma of primitive gonads and in the esophageal submucosa at the stage with external gills.<sup>18,19</sup>

The epigonal organ of cartilaginous dogfish is associated with the mesentery in which the gonad develops. It appears at the egg case splitting stage (6 months) and develops more slowly than the Leydig organ. At later stages (8 months and onward) the cell density is less compact than at earlier stages.<sup>17</sup>

A dimensional hematopoietic cell relationship exists between the Leydig and epigonal organs: if one is absent, the other is usually very large.<sup>20</sup> Granulopoietic tissue mainly occurs in these organs and it was reported that active erythropoiesis can be identified in the Leydig organ of the basking shark *Cetorhinus maximus* and other elasmobranchs after splenectomy.<sup>21-23</sup>

McClusky *et al.*<sup>24</sup> reported that the leukocytes of the lymphomyeloid epigonal organ are involved in the phagocytosis of unwanted cells in the blue shark *Prionace glauca*. Andreyeva *et al.*<sup>25</sup> studied the hematopoietic organs of black scorpionfish (*Scorpaena porcus*) by flow cytometry and light microscopy: they observed "small cells" subpopulation in spleen and kidney whose morphological and functional features correspond to colony-forming units of mammals and are precursor pluripotent hemopoietic cells of teleosts.

The HSC in mammals is characterized by CD34 antigen expression and selected CD34 positive (CD34+) cells used for clinical stem cell transplantation. Recent reports indicate that the most primitive HSC may be CD34 negative (CD34-) and the expression of growth factor receptors in these cells suggests that CD34- stem cells are probably

more quiescent than CD34+ stem cells.<sup>26</sup> CD34 is a transmembrane phosphoglycoprotein and its commonly cited ligand is L-Selectin, together with the adapter protein CrkL, also known for adhesion to CD34.<sup>27</sup> Sidney *et al.*<sup>27</sup> reported that CD34 is expressed by progenitor cells from larger cell populations, including mesenchymal cells, and is not associated solely with hematopoietic and endothelial cells. In human embryos, CD34+ cells originate in the yolk sac and they are detected in the bone marrow at approximately 14 weeks of gestation.<sup>28</sup> There no information concerning the expression of CD34 in HSCs of the elasmobranchs but it was indirectly demonstrated the occurrence of circulating HSCs in the marbled electric ray by the hemopoietic regeneration of the spleen and lymphomyeloid tissues, after sublethal X-irradiation followed by autohemotransplantation.<sup>29</sup>

Cells bearing the CD34 antigen have been detected in other aquatic species. This assemblage includes the hemoblasts of the bivalve mollusk *Tapes philippinarum*<sup>30</sup>, hematopoietic cells of the bone marrow and kidney of *Lithobates catesbeianus*<sup>31</sup> and in a *Conger conger* angioleiomyoma<sup>32</sup>, all using antimouse CD34 monoclonal antibody.<sup>32</sup>

To date the CD34+ debut was demonstrated in mammalian yolk sac,<sup>33</sup> but no data have been reported about the occurrence of hematopoietic stem cells in extraembryonic annexes of cartilaginous fishes.

Hamlett *et al.*<sup>34</sup> investigated the development of the umbilical cord and placenta in the Atlantic sharpnose shark *Rhizoprionodon terraenovae*. When their embryos are 4.0 cm in length, the yolk stalk differentiates into an elongate umbilical cord, that includes a muscular umbilical artery and umbilical vein separated by the ductus vitellointestinalis and the extraembryonic coelom. The body of the core is supplied by small blood vessels and by appendiculae. Columnar cells of the appendiculae with bulging luminal apices are covered with elongated microvilli and contain prominent lipid inclusions.

The objective of this study is to trace the temporal and structural development of the lymphomyeloid tissues during embryonic development of the *Torpedo marmorata* and the debut of CD34+ HSCs in these loci. This investigation, along with companion studies,<sup>35</sup> is thus designed to document the evolutionary initiation of the appearance and the site of origin of the hemopoietic stem cell in the most basal vertebrate model, *i.e.* the chondrichthyan, in which a complete functional vertebrate skeleton, an intact, closed circulation with passively circulating leukocytes and erythrocytes in the adult animal are expressed.

## Materials and Methods

Three embryonic stages of torpedoes were studied. The embryos were removed by cesarean section from a total of six pregnant torpedoes (3 *Torpedo marmorata* Risso and 3 *Torpedo ocellata* Rafinesque). Three embryos per stage were used. In addition, four adult torpedoes (two male and two female) and the bone marrow of two newborn rats were used as controls. All the torpedoes, caught in the Gulf of Naples during June to October, were kindly provided by the Zoological Station A. Dohrn (Naples, Italy). The characteristics of the subjects are summarized in Table 1.

All the specimens were narcotized with MS222, 62 mg/L (Sigma, St Louis, MO, USA). The embryos of pregnant torpedoes (1-5 of Table 1) were fixed *in toto*. The esophagi and the gonads surrounded by the epigonal tissue were taken from embryos of the torpedo n. 6 and from the adult specimens. The experiments were performed under institutional approval and all efforts were made to avoid animal suffering. The yolk sac was studied in the sections of stage II embryos.

## Histology

Some embryos at stages I (n=3), esophagi from embryos at stage III (n=3) and esophagi from adult animals (n=2) were fixed in Bouin's solution (40% formaldehyde, saturated picric acid solution and glacial acetic acid, 5:15:1) for 48h and washed in ethanol 75% and lithium carbonate.

Other embryos at stage I (n=3), esophagi from embryos at stage III (n=3) and esophagi from adult animals (n=2) were perfused with fixative solution (4% paraformaldehyde, Sigma, in PBS) for 1h. The narcotized animal pericardial cavity was opened and the common cardinal veins were severed, to allow the blood to escape. Subsequently, using the 2 cm butterfly needle, physiologic saline solution was injected to obtain the complete evacuation of the vessels. The fixative was slowly administered and the amount utilized was proportional to a given animal's dimensions. After the perfusion of the narcotized subject, its esophagus was removed, immersed for another 6 hours in the fixative solution and washed in 0.1 M phosphate buffer, pH 7.4.

Lymphomyeloid tissue surrounding gonads, called epigonal organ, displays a morphology identical to that of esophageal tissue. Consequently the methods used in this study were applied mainly on esophageal tissue.

## Paraffin embedding and sectioning

The samples were dehydrated using

ascending grades of alcohol (75% ethanol, 95% ethanol for 24 h) (2 changes), ethanol 100% for 45 min (3 changes). All samples were embedded in methylbenzoate (Carlo Erba, Cornaredo, MI, Italy), clarified in benzene (Carlo Erba) for 10 min (2 changes) and immersed in liquid paraffin, in an oven at 58°C overnight and under vacuum. Sections of the paraffin-embedded tissue blocks (embryos and esophagi) were cut at a thickness of 4-10 µm in series, each consisting of three adjacent sections: the first was processed for double immunocytochemistry, the second for a negative control and the third was stained with the Galgano trichromic method or hemalum-eosin.

Blood smears were prepared using blood from the caudal vessels and stained with the May-Grünwald-Giemsa stain (MGG).

### Double immunocytochemistry

The double immunolabeling reaction was performed to identify the presence of CD34 and CD38 antigens on the surface of hemopoietic progenitor cells. Each histological section of isolated embryo and of esophagus was treated sequentially with 2 types of antibody: monoclonal anti-CD34 antibody (mouse anti-human, clone QBEnd/10; Novocastra Laboratories Ltd., Newcastle upon Tyne, UK) - in agreement with de Abreu Manso *et al.*<sup>31</sup> and Marino *et al.*<sup>32</sup> who used the same clone to identify CD34+ cells respectively in bullfrog and in conger - followed by secondary biotinylated antibody (horse anti-mouse IgG, BA-2000 Vector Laboratories, Inc., Burlingame, CA, USA) labeled with peroxidase (HRP-DAB method detection) or followed by protein A marked with colloidal gold (immunogold detection) and polyclonal anti-CD38 antibody (goat IgG polyclonal, M-19, sc-7049; Santa Cruz Biotechnology, Inc., Santa Cruz, CA, USA) followed by secondary antibody (goat anti-rabbit IgG-AP, sc-

2007; Santa Cruz) labeled with alkaline phosphatase whose detection shows an intense red color. Imprints of newborn rat bone marrow were used as positive controls. As negative controls, some sections were processed with the same protocol omitting the primary antibody; no immunostaining was detected in these preparations, as reported in Manca *et al.*<sup>35</sup>

The samples were deparaffinized in xylene I and xylene II (fifteen min each) and rehydrated in decreasing concentrations of alcohol (ethanol 100%, 95%, 75% and 50%, five min for each). The high temperature antigen unmasking technique was performed using citrate buffer and a microwave oven (MW 310; DeLonghi, Treviso, Italy). The sections, mounted on slides, were incubated in 10 mM citrate buffer, pH 6.0, in capped plastic jars, placed in water and microwaved at 400 W (4 treatments for 5 min each); the slides were then kept in citrate buffer at room temperature for 20 min. After washing in 0.1 M phosphate-buffered saline, pH 7.4 (PBS), the sections were treated for 1 h in 0.5N HCl at 37°C, washed for 3 times in distilled water and in Sorensen glycine solution (42.4 mL of HCl 0.1 N + 57.6 mL of 0.2 M glycine solution, pH 2.2) for 2 h at 37°C.

The samples were washed in distilled water, in PBS and then labeled with alkaline phosphatase, peroxidase and colloidal gold. The sections labeled with peroxidase and colloidal gold were counterstained with Mayer's hemalum solution dehydrated and mounted in Eukitt.

### Alkaline phosphatase labeling

The sections were incubated for 1h in blocking solution, performed with 5% normal goat serum NGS (Vector) in PBS, and incubated overnight, in a humid chamber at 4°C, with primary antibodies that recognize CD38 antigen (goat IgG polyclonal, M-19, sc-7049, Santa Cruz US), diluted 1:100 in

normal goat serum (NGS, Dako, Glostrup, Denmark). After several rinses, the samples were incubated for 2 h in secondary antibody (goat anti-rabbit IgG-AP, sc-2007, Santa Cruz), diluted 1:50 in NGS, and washed in Tris-HCl 0.1 M, pH 8.2-8.5 for 5 min. The sections were treated with levamisole solution (Levamisole, Vector, and 5 mL of Tris-HCl, pH 8.2) for 15 min to inactivate endogenous phosphatase activity, and washed in Tris-HCl 0.1 M, pH 8.2-8.5 for 5 min. The sections were incubated in alkaline phosphatase Kit working solution (Vector) for 15 min in the dark and washed with Tris-HCl pH 8.2 followed by distilled water, 5 min each.

### Peroxidase labeling

The sections were treated for 15 min in 3% H<sub>2</sub>O<sub>2</sub> to inactivate endogenous peroxidase, washed in PBS for 3 times for 5 min each and incubated for 1h at room temperature with 5% normal horse serum (NHS; Vector) in PBS. Subsequently, the samples were incubated overnight in a humid chamber at 4°C, with primary antibodies anti-CD34 (mouse anti-human, clone QBEnd/10; Novocastra), diluted 1:25 in NHS. After several washings, the samples were incubated in secondary biotinylated antibody (horse anti-mouse IgG, BA-2000; Vector) in NHS (1:12.5), followed by avidin-biotin-peroxidase labeling (ABC Kit, Vectastain; Vector), as reported by Manca *et al.*<sup>35</sup>

### Immunogold labeling

The sections were blocked for 30 min in distilled water containing 1% bovine serum albumin (BSA) and 0.15% glycine, and incubated overnight in anti-CD34 antibody (mouse anti-human, clone QBEnd/10; Novocastra) in BSA 1:25 at 4°C. After several washing, the samples were incubated in BSA 1% for 15 min, followed by further incubation with 20 nM of protein A, diluted

**Table 1. Characteristics of the specimens.**

Pregnant torpedo	Capture month	Total length	Weight	Total n of embryos	Embryo shape	Embryo size	Yolk sac
1	Mid-June	25 cm	1 kg	8	Flattened	2.7-3.5 cm	External
2	End of June	30 cm	1.5 kg	12	Elongated	2 cm	External
3	Early July	36 cm	2 kg	9	Flattened	3.7 cm	External
4	Mid-July	50 cm	2.5 kg	12	Flattened	3.8-4.8 cm	External
5	October	35 cm	1.6 kg	7	Flattened	6-8 cm	External
6	October	50 cm	2.8 kg	14	Flattened	11 cm	Resorbed
Adult torpedo	Capture month	Total length	Weight				
1	Mid-June	20 cm	180 g				
2	Mid-June	20 cm	220 g				
3	Mid-June	20 cm	330 g				
4	Mid-June	20 cm	800 g				

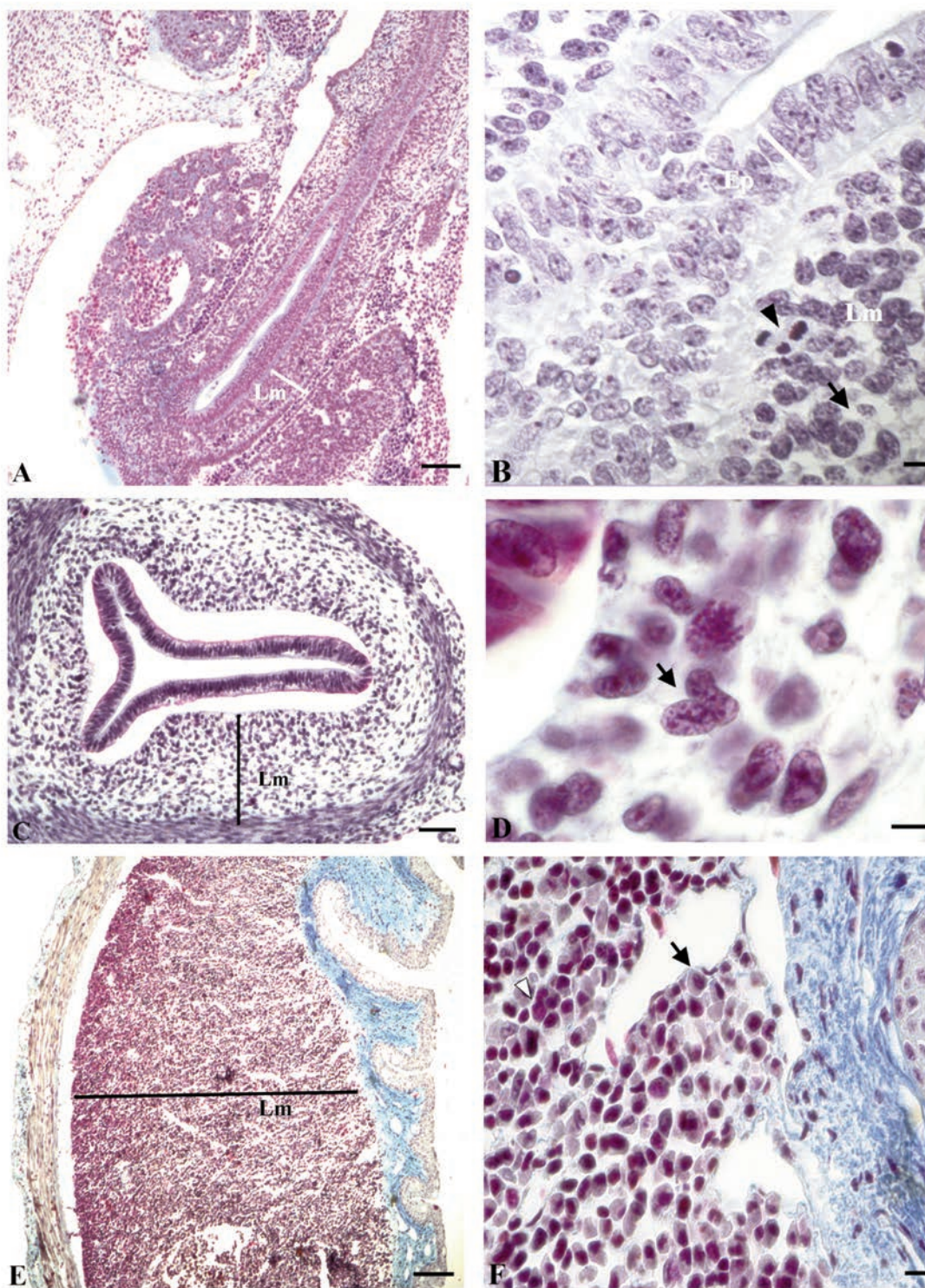


Figure 1. A) Sagittal section of esophagus of *Torpedo marmorata* Risso embryo at stage I (not flattened, total length 2 cm, external gill filaments). Galgano's trichromic stain; lymphomyeloid tissue (Lm) appears as a thick band in the submucosa around the esophagus, up to the cranial part of the stomach; the tissue close to the epithelium circumscribes a central lumen; scale bar: 7.8  $\mu$ m. B) Lymphoid-like cells (arrow) in the area below the lining epithelium (Ep) of the esophagus, star-like mesenchymal cells, close to the external esophageal wall, and several cells in mitosis (arrowhead); scale bar: 6.5  $\mu$ m. C) Cross section of esophagus of *Torpedo marmorata* Risso embryo at stage II (flattened embryo, total length 3.2 cm); Galgano's trichromic stain; lymphoid-like cells located below the lining epithelium of the esophageal canal and mesenchymal cells in the peripheral region are distinguishable; the muscular layer and the external epithelial wall are in the peripheral zone; scale bar: 7.8  $\mu$ m. D) Mitosis of lymphoid-like cells (arrow); scale bar: 6.5  $\mu$ m. E) Sagittal section of esophagus of *Torpedo marmorata* Risso embryo at stage III (flattened, total length 11cm, ready to be born with completely reabsorbed yolk sac); Galgano's trichromic stain; the lymphomyeloid tissue (Lm) is located between the connective tissue (blue) and the external muscular layer; scale bar: 7.8  $\mu$ m. F) Neutrophil myelopoiesis (arrow) and eosinophilic myelopoiesis (white arrowhead) are observed; scale bar: 6.5  $\mu$ m.

in BSA 1%. After several rinses, the antibody complexes were revealed by treatment for 10 min with silver enhancer (Sigma-Aldrich, Darmstadt, Germany), rinsing in 2.5% sodium thiosulphate solution followed by distilled water.

## Results

### Developing and mature lymphomyeloid tissue morphology

Embryos were classified as stages I, II, III according to their structural presentation, as reported by Manca *et al.*<sup>35</sup>

#### Stage I

At this stage the esophageal wall extends under an epithelium of cylindrical cells. A thickening of the future lymphomyeloid tissue is already evident in its ventral and dorsal regions (Figure 1A). Cells characterized by a spherical shape, central nucleus, and homogeneous nongran-

ulated, lightly stained cytosol classifiable as lymphoid type cells are observed in the epithelium that circumscribes the central lumen of this organ. Star-like mesenchymal cells, close to the external esophageal wall, and several cells in mitosis are evident (Figure 1B).

#### Stage II

Transverse sections of trichrome-stained esophagus display three anatomical, cytologic layers. These are an inner layer of lymphoid-like cells near the lumen, an adjacent layer containing mesenchymal cells and a peripheral muscular layer followed by an external epithelial wall (Figure 1 C,D).

The external yolk sac detected at this stage appears as a cordlike structure, containing blood vessels full of megalocytes and yolk drops dispersed around the vessels. CD34+/CD38- cells were rarely detected among megalocytes (Figure 2).

#### Stage III

The sagittal sections of the esophagus at

stage III, stained by the trichromic method, display connective tissue which is located between the epithelium and the lymphomyeloid tissue. The aggregate of the latter tissue is a rather thickened mass (Figure 1 E,F). Its assemblage of cells is similar to that obtained in adult torpedoes, *i.e.*, both myeloid and lymphoid cells at different levels of maturation are identifiable (Figure 3). In particular the eosinophilic granulocytopenesis and a modest amount of neutrophilic granulocytopenesis are seen. Lymphocytopenesis occurs in small clusters of cells. These cells are characterized by a spherical shape and have a diameter of approximately 18  $\mu\text{m}$ . They have a high nuclear-cytoplasmic ratio, an intensely basophilic cytoplasm, and the nucleus presents a reticular chromatin network along with nucleoli. This cytologic morphology suggests that these cells are HSCs (Figure 4 A,B).

#### Adult

Adult lymphomyeloid tissue structure

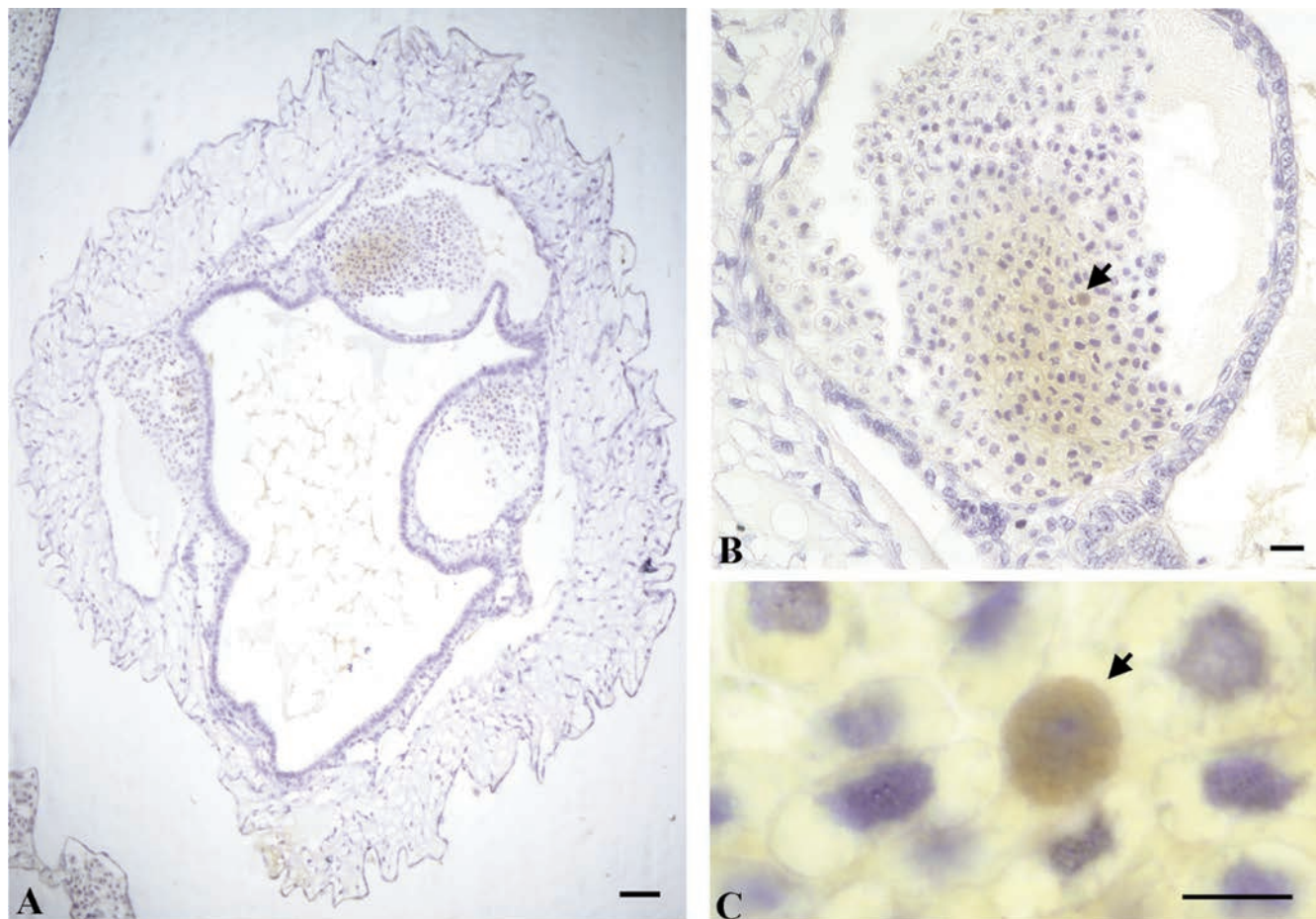


**Figure 2.** Immunostaining of consecutive sagittal sections of the external yolk sac of a stage II embryo (flattened embryo, total length 3.2 cm). A) Transverse section of external yolk sac showing the vessels full of megalocytes and area with dispersed yolk drops. Double immunostaining CD34-HRP-DAB/CD38-ALP; scale bar: 10  $\mu\text{m}$ . B) Detail of panel A; CD34+/CD38- cell was detected (arrow); scale bar: 11  $\mu\text{m}$ . C) CD34+/CD38- cell among megalocytes in a vessel (arrow); scale bar: 15  $\mu\text{m}$ .

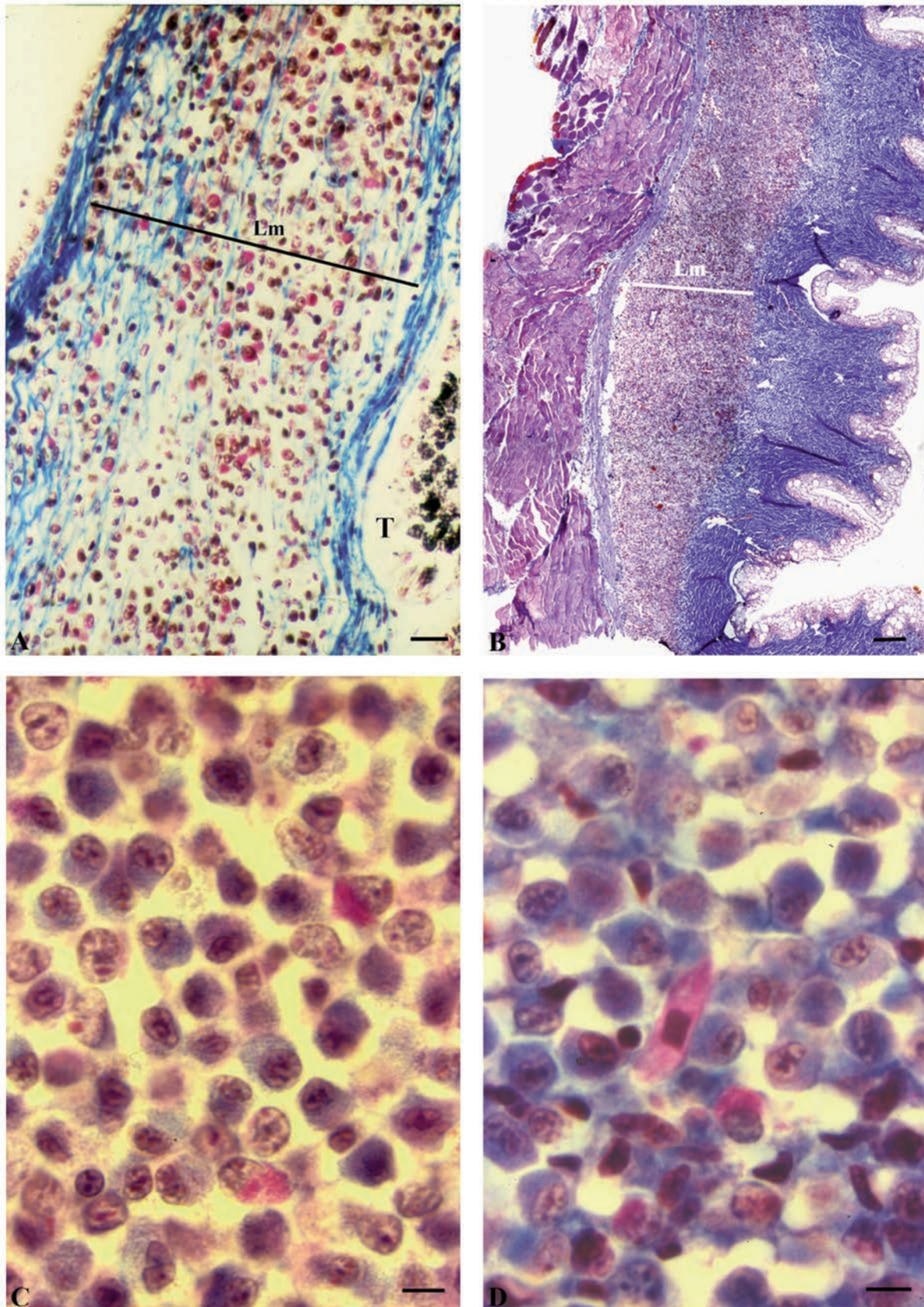
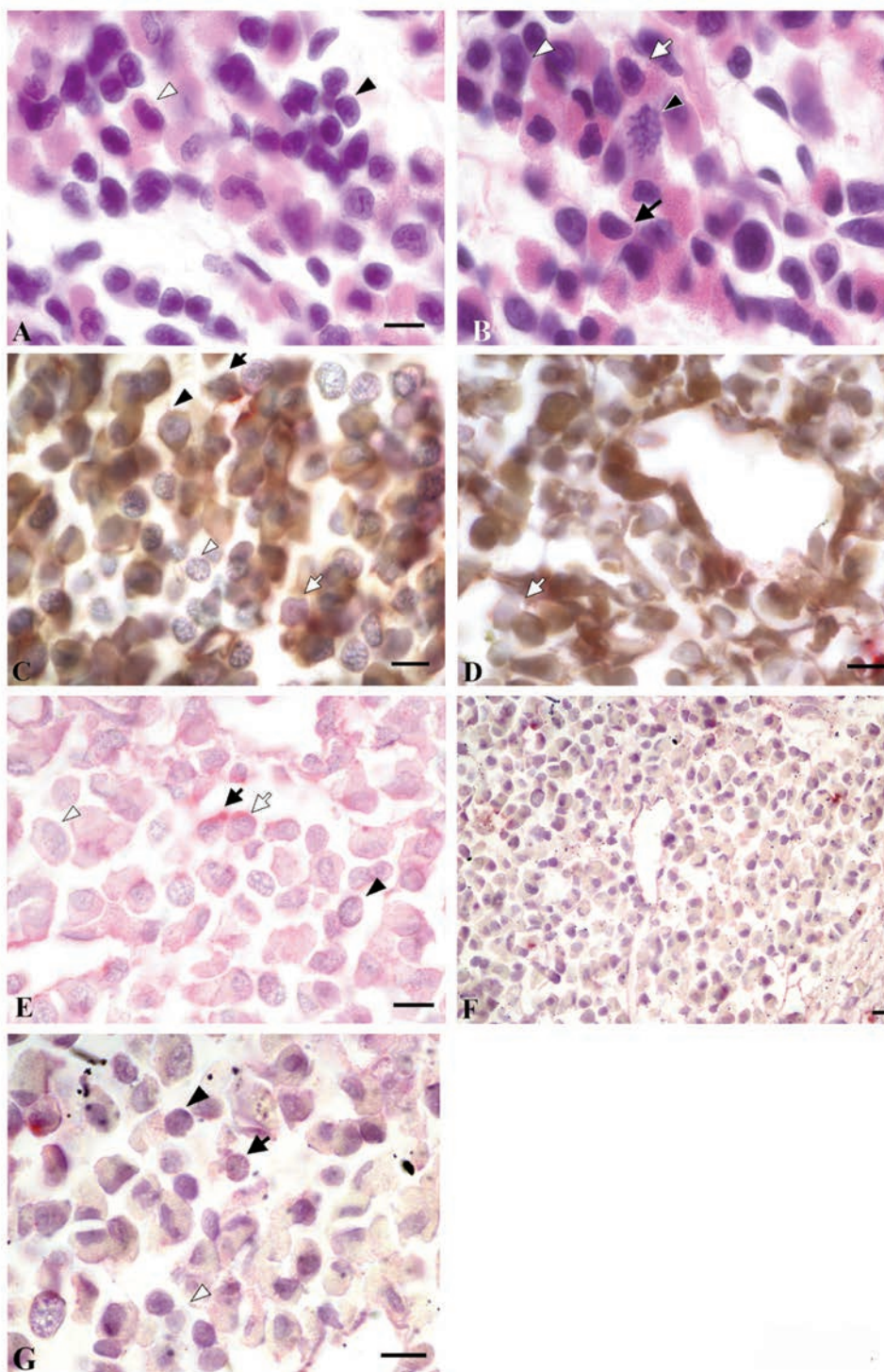


Figure 3. Sagittal sections of epigonal and Leydig organs of adult *Torpedo marmorata* Risso. A) Lymphomyeloid (Lm) epigonal tissue, surrounding testis, below a part of seminiferous tubule (T) showing spermatozoa; Galgano's trichromic stain; scale bar: 10  $\mu$ m. B) Lymphomyeloid (Lm) Leydig tissue, between the connective tissue (blue) and the external muscular layer; Galgano's trichromic stain; scale bar: 22  $\mu$ m. C,D) Granulocytopenia in epigonal and Leydig lymphomyeloid tissues, respectively; scale bar: 6.6  $\mu$ m.



**Figure 4.** Sagittal sections of esophagus of *Torpedo marmorata* Risso embryo at stage III (flattened, total length 11cm, ready to be born with completely reabsorbed yolk sac). **A)** Hemalum-eosin stain. The figure shows cells in various maturation stages, in particular metamyelocytes (white arrowhead) and locus of lymphocytopoiesis (black arrowhead); scale bar: 6.6  $\mu$ m. **B)** Myeloid cells at various stages of maturation, in which there are myeloblasts (white arrowhead), myelocytes (white arrow), metamyelocytes (black arrow) and a myeloid cell in mitosis (black arrowhead); no stem cells are detectable with histological staining; scale bar: 6.6  $\mu$ m. **C, D)** Double immunostaining CD34-HRP-DAB/CD38-ALP of sections from an embryonic esophagus of stage III; in this section several cell populations can be observed: CD34+/CD38-cells (brown-stained immunoreactivity, black arrowhead), CD34+/CD38+cells (red and brown stained cytoplasm, black arrow), CD34-/CD38+cells (red stained cytoplasm, white arrow), CD34-/CD38-cells (blue, as contrast staining to Hemalum-eosin, white arrowhead); scale bar: 6.6  $\mu$ m. **E)** Double immunogold staining CD34-colloidal gold-S.E./CD38-ALP. Four cell phenotypes are observed in this section: CD34+/CD38- (black arrowhead), CD34+/CD38+ (black arrow), CD34-/CD38+ (white arrow) and CD34-/CD38- (white arrowhead). scale bar: 6.6  $\mu$ m. **F)** Lymphomyeloid tissue and lymphocytopoiesis; scale bar: 4  $\mu$ m. **G)** Three cell phenotypes are observed: CD34+/CD38-cells (black arrowhead), CD34+/CD38+cells (black arrow), CD34-/CD38-cells (white arrowhead); scale bar: 6.6  $\mu$ m.

has been previously described by Pica and Della Corte.<sup>13</sup> The epigonal organ is a yellowish-white irregular shaped mass located in the mesenteric folds of the gonads. In the adult torpedo the volume of epigonal tissue is decreased in relation to the increased size of the gonads. The tissue is more compact and less lobulated than the Leydig organ (Figure 3A). The Leydig's organ is composed of two lobes, ventral and dorsal, which are located between the mucosa and muscular strata of the esophagus. It contains irregular venous sinuses and a small number of arteries (Figure 3B).

The Leydig and epigonal organs have a very similar cellular composition. They contain granulocytes in different stages of maturation, various types of non-granulated cells with a basophilic cytoplasm, lymphocytes, occasional plasma cells, and some presumed blast cells. The most common granulocyte is the eosinophil. Lymphocytes are distributed throughout the tissues but they also form nodule-like aggregations, especially in the epigonal organ. Many of the developing granulocytes are identifiable as to their specific level of maturity, i.e. promyelocytes, myelocytes and metamyelocytes. As would be expected their nuclei became condensed, lobed, and decreased in volume with maturation (Figure 3 C,D).

### Immunocytochemical findings

Neither CD34+ nor CD38+ cells are identifiable in lymphomyeloid tissues of stage I and stage II embryos. However, some lymphoid-like cells that do not demonstrate any immunolabeling for these antibodies are present. In the stage II embryo yolk sac, rare CD34+CD38- cells were identified (Figure 2).

In stage III embryo the lymphomyeloid tissues display the following cell populations, CD34+CD38-, CD34+CD38-, CD34-CD38+, and CD34-CD38- (Figure 4).

The lymphoid-like cells described as probable stem cells in the above morphological description, present a CD34+CD38- phenotype, as evidenced by brown staining with DAB (Figure 2 and Figure 4 C,D). These are CD34 immunopositive after the double immunogold labeling (Figure 4E). These qualities suggest that they are progenitors of the HSC. The double immunostained documented CD34+CD38+ population includes maturational stages of the lymphoid series (including lymphoblasts and further developed forms). The CD34-CD38+ immunoreactive cells (stained red by the ALP technique) express only the CD38 antigen and are believed to be pro-lymphocytes. The CD34-CD38- phenotype includes all differentiated stages of the myeloid (eosinophils and neutrophils) and lymphoid series (Figure 4 F,G).

### Discussion

The exposure of HSCs to different extracellular microenvironments supports their development and maturation.<sup>36</sup> The cellular and environmental regulation of hematopoiesis has been generally conserved throughout vertebrate evolution.<sup>1</sup> The development of differentiated hematopoietic cells involves a series of lineage decisions that are driven by the activity of multiple key transcription factors. Hematopoietic development is controlled in a temporal, spatial, and molecular manner, and despite subtle differences in their origin, the genetic programs that regulate each distinct wave are highly conserved between fishes and mammals.<sup>37,38</sup>

It has been hypothesized that the HSCs engraftment occurs in the bone marrow of terrestrial animals in order to confer protection from ionizing radiation, fulfilling the protective role of water.<sup>39</sup> Kapp *et al.*<sup>40</sup> detected the presence of melanocytes in hematopoietic kidney of zebrafish. These cells form an opaque shield dorsal to the kidney to protect the DNA of the HSCs from UV-induced degradation. In fact, HSCs isolated from the irradiated unpigmented larvae showed higher levels of damage DNA. Moreover, consistent with this observation, mutants that lack melanocytes had normal steady-state hematopoiesis under standard laboratory conditions. The protective role of melanocytes associated with the hematopoietic niche is highly evolutionarily conserved in aquatic animals. Melanocytes covering the hematopoietic kidney have been discovered in many teleosts (*Ictalurus punctatus*, *Gasterosteus aculeatus*, *Lepomis macrochirus* and *Lepomis microlophus*), in chondrostei (*Acipenser fulvescens*) and in holostei (*Atractosteus spatula*). The analysis of the amphibian *Dendrobates tinctorius*'s hematopoietic niche revealed a transition from a melanocyte-covered niche to the bone marrow during its aquatic environmental development of its legs.<sup>40</sup>

The hematopoietic cell development occurs in two distinct regions of the vertebrate embryo: the yolk sac and the intraembryonic mass. It still remains an open question as to which tissue leads to the development of the hematopoietic system in the adult mammal. Studies of non-mammalian embryos have generated the proposal that the intraembryonic mass autonomously generates the first adult HSCs and strongly suggest that the mammalian embryo body gives rise to the definitive adult hematopoietic system.<sup>7</sup> Current thinking supports the concept that future endeavors will identify specific cells as the progenitors of hemo-

poiesis. The occurrence of CD34+CD38-HSC in the torpedo yolk sac, observed in the present study, demonstrates the unity of the sites of early hemopoiesis in cartilaginous fishes, teleosts and all other vertebrates<sup>1</sup>. Subsequently, the spleen and both esophageal and epigonal lymphomyeloid tissues became the principal sites for the development of hematopoietic progenitors in embryonic *Torpedo marmorata* Risso. Erythroid, lymphoid, and thrombocytic genesis and differentiation occur in the spleen while myelopoiesis and a small portion of lymphocytopoiesis initiate in both esophageal and epigonal lymphomyeloid aggregate. As would be anticipated both organs undergo various morphological changes during embryonic development. The lymphomyeloid organs house some lymphoid-like cells in the area close to the central lumen, along with a prevalence of mesenchymal cells in the periphery during the torpedo's stage I of embryonic development. Neither CD34 or CD38 immunoreactive cells are identifiable in the esophageal and epigonal tissue while CD34+CD38- cells were identified in external yolk sac, during the embryonic stage II. Therefore the hemopoiesis of embryonic stage II is still extraembryonic.

The stage III embryos examined in this investigation presented esophageal and epigonal lymphomyeloid tissues that were hematopoietically advanced and very similar to that of the adult. In particular, the CD34/CD38 double labeling revealed the presence of four hematopoietic cell populations. The most immature cells have a phenotype CD34+CD38-. The successive maturation stages express the immunopositivity for CD34+CD38+; by maturation CD34 disappears and the cells express only CD38 (CD34-CD38+). The differentiated lymphocytes and granulocytes present none of this immunoreactivity (CD34-CD38-).

Consequently, it is possible to recognize a gradient of CD34 immunoreactivity. It is identifiable in the most immature recognizable forms and its expression decreases in maturing cells until its complete disappearance in differentiated cells. It is pertinent to recognize the related phenomenon obtained in mammals that in concert with mammalian embryo maturation a progressive reduction of CD34 expression occurs along with an increasing expression of another markers, i.e., CD38.<sup>41,42</sup> It is documented that the expression of CD34 on hematopoietic progenitor cells and its extraembryonic origin, in the yolk sac, is conserved along the evolutionary scale. Conservation of antigenic protein occurred through phylogenetic development. Several studies corroborate the protein conservation between most basal vertebrates and mammals (clam *Tapes*



*philippinarum*,<sup>30</sup> bullfrog *Lithobates catesbeianus*,<sup>31</sup> conger *Conger conger*,<sup>32</sup> sea bass *Dicentrarchus labrax*,<sup>43,44</sup> teleosts,<sup>45</sup> bony fish *Dicentrarchus labrax*,<sup>46</sup> dogfish *Scyliorhinus canicula*<sup>47</sup>). This is not surprising in evo-devo era, on the basis of the increasing evidences of evolutionary conserved genes, playing a role in generating the biological form, from invertebrates to mammals.<sup>48</sup>

The CD34 antigen is identifiable in the earliest full-fledged elasmobranchs up to including Mammalia, based on the fact that at least one epitope of this antigen is recognized by antibodies to mammalian cells.

## References

- Zon Li. Developmental biology of hematopoiesis. *Blood* 1995;86:2876-91.
- Dzierzak E, Medvinsky A, de Bruijn M. Qualitative and quantitative aspects of haematopoietic cell development in the mammalian embryo. *Immunol Today* 1998;19:228-36.
- Tavian M, Coulombel L, Luton D, Clemente HS, Dieterlen-Lievre F, Peault B. Aorta-associated CD34+ hematopoietic cells in the early human embryo. *Blood* 1996;87:67-72.
- Tavian M, Hallais MF, Peault B. Emergence of intraembryonic hematopoietic precursors in the pre-liver human embryo. *Development* 1999;126:793-803.
- Barcena A, Muench MO, Kapidzic M, Fisher SJ. A new role for the human placenta as a hematopoietic site throughout gestation. *Reprod Sci* 2009;16:178-87. doi: 10.1177/1933719108327621.
- Ivanovs A, Rytsov S, Ng ES, Stanley EG, Elefanty AG, Medvinsky A. Human haematopoietic stem cell development: from the embryo to the dish. *Development* 2017;144:2323-37. doi: 10.1242/dev.134866.
- Dzierzak E. Hematopoietic stem cells and their precursors: developmental diversity and lineage relationships. *Immunol Rev* 2002;187:126-38.
- Medvinsky A, Dzierzak E. Definitive hematopoiesis is autonomously initiated by the AGM region. *Cell* 1996; 86:897-906.
- Willett CE, Cortes A, Zuasti A, Zapata AG. Early hematopoiesis and developing lymphoid organs in the zebrafish. *Dev Dyn* 1999;214:323-36.
- Tian Y, Xu J, Feng S, He S, Zhao S, Zhu L, et al. The first wave of T lymphopoiesis in zebrafish arises from aorta endothelium independent of hematopoietic stem cells. *J Exp Med* 2017;214:3347-60. doi: 10.1084/jem.20170488.
- de Pater E, Trompouki E. Bloody zebrafish: Novel methods in normal and malignant hematopoiesis. *Front Cell Dev Biol* 2018;6:124. doi: 10.3389/fcell.2018.00124.
- Kobayashi I, Katakura F, Moritomo T. Isolation and characterization of hematopoietic stem cells in teleost fish. *Dev Comp Immunol* 2016;58:86-94. doi: 10.1016/j.dci.2016.01.003.
- Pica A, Della Corte F. Hemopoiesis, lymphomyeloid tissues, spleen and thymus of Torpedoes: in normal conditions and after treatment with cobamamide and folic acid. *Arch Ital Anat Embr* 1987;92:249-61.
- Mattison A, Fänge R. The cellular structure of the Leydig organ in the shark, *Etmopterus spinax* (L.). *Biol Bull* 1982;162:182-94.
- Pica A, Grimaldi MC, Della Corte F. The circulating blood cells of Torpedoes (*Torpedo marmorata* Risso and *Torpedo ocellata* Rafinesque). *Monit Zool Ital - Ital J Zool* 1983;17: 353-374.
- Fänge R. Lymphomyeloid system and blood cell morphology in elasmobranchs. *Arch Biol (Bruxelles)* 1987;98:187-208.
- Lloyd-Evans P. Development of the lymphomyeloid system in the dogfish, *Scyliorhinus canicula*. *Dev Comp Immunol* 1993;17:501-14.
- Zapata AG, Torroba M, Sacedón R, Varas A, Vicente A. Structure of lymphoid organ of elasmobranchs. *J Exp Zool* 1996;275:125-43.
- Navarro R. [Ontogenia des organos linfoides de *Scyliorhinus canicula*. Estudio ultrastructural]. [Thesis in Spanish]. Universidad Complutense, Madrid, 1987.
- Fänge R. [Lymphomyeloid tissues in fishes]. [Article in Danish]. *Vidensk Meddr dansk naturh Foren* 1984;145:143-62.
- Matthews LH. Reproduction in the basking shark *Cetorhinus maximus*. *Philos T R Soc B* 1950;234:247-315.
- Drzewina A. Contribution d l'etude du tissue lympholde des Ichthyopsides. *Archs Zool Exp Gen* 1905;4:145-338.
- Fänge R, Johansson-Sjöbeck ML. The effect of splenectomy and the hematolgy and on the activity of 6- amino-levulinic acid dehydratase (ALA-D) in hemopoietic tissues of the dogfish *Scyliorhinus canicula* (Elasmobranchi). *Comp Biochem Physiol* 1975;52A:577-80.
- McClusky LM, Sulikowski J. The epigonal organ and mature pole of the testis in the recreationally fished blue shark (*Prionace glauca*): histochemico-functional correlates. *J Anat* 2014;225:614-24. doi: 10.1111/joa.12242.
- Andreyeva AY, Soldatov AA, Kukhareva TA. Black scorpionfish (*Scorpaena porcus*) hemopoiesis: Analysis by flow cytometry and light microscopy. *Anat Rec (Hoboken)* 2017;300:1993-9. doi: 10.1002/ar.23631.
- Donnelly DS, Krause DS. Hematopoietic stem cells can be CD34+ or CD34-. *Leuk Lymphoma* 2001;40:221-34. doi: 10.3109/10428190109057921.
- Sidney LE, Branch MJ, Dunphy SE, Dua HS, Hopkinson A. Concise review: evidence for CD34 as a common marker for diverse progenitors. *Stem Cells* 2014;32:1380-9. doi: 10.1002/stem.1661.
- Allen JE, Henshaw DL. An in situ study of CD34(+) cells in human fetal bone marrow. *Br J Haematol* 2001;114:201-10.
- Pica A, Cristino L, Sasso FS, Guerriero P. Haemopoietic regeneration after autohaemotransplant in sublethal X-irradiated marbled electric rays. *Comp Haematol Int* 2000;10:43-9. doi: 10.1007/s005800070026.
- Cima F, Matozzo V, Marin MG, Ballarin L. Haemocytes of the clam *Tapes philippinarum* (Adams & Reeve, 1850): morphofunctional characterisation. *Fish Shellfish Immunol* 2000;10:677-93. doi: 10.1016/j.cellbi.2008.03.008.
- de Abreu Manso PP, de Brito-Gitirana L, Pelajo-Machado M. Localization of hematopoietic cells in the bullfrog (*Lithobates catesbeianus*). *Cell Tissue Res* 2009;337:301-12. doi: 10.1007/s00441-009-0803-0.
- Marino F, Licata L, Albano M, Ieni A, Di Caro G, Macrì B. Angioleiomyoma in a conger (*Conger conger*). *Dis Aquat Organ* 2016;119:85-9. doi: 10.3354/dao02984.
- Yoder MC, Hiatt K, Dutt P, Mukherjee P, Bodine DM, Orlic D. Characterization of definitive lymphohematopoietic stem cells in the day 9 murine yolk sac. *Immunity* 1997;7:335-44.
- Hamlett WC, Miglino MA, Federman DJ, Schafer PJ, Didio LJ. Fine structure of the term umbilical cord in the Atlantic sharpnose shark, *Rhizoprionodon terraenovae*. *J Submicrosc* 1993;5:547-57.
- Manca R, Glomski CA, Pica A. Evolutionary intraembryonic origin of vertebrate hematopoietic stem cells in the elasmobranch spleen. *Eur J Histochem* 2018;62:2987. doi: 10.4081/ejh.2018.2987.
- Wang LD, Wagers AJ. Dynamic niches

- in the origination and differentiation of haematopoietic stem cells. *Nat Rev Mol Cell Biol* 2011;12:643-55. Erratum in: *Nat Rev Mol Cell Biol* 2011;13:12. doi: 10.1038/nrm3184.
37. Robertson AL, Avagyan S, Gansner JM, Zon LI. Understanding the regulation of vertebrate hematopoiesis and blood disorders - big lessons from a small fish. *FEBS Lett* 2016;590:4016-33. doi: 10.1002/1873-3468.12415.
38. Ciau-Uitz A, Monteiro R, Kirmizitas A, Patient R. Developmental hematopoiesis: ontogeny, genetic programming and conservation. *Exp Hematol* 2014;42:669-83. doi: 10.1016/j.exphem.2014.06.001.
39. Cooper EL, Klempau AE, Ramirez JA, Zapata AG. Source of stem cells in evolution. In: Horton JD, Editor, *Development and differentiation of lymphocytes in vertebrates*. Elsevier North-Holland Biomedical Press, Amsterdam; 1980; pp. 3-11.
40. Kapp FG, Perlin JR, Hagedorn EJ, Gansner JM, Schwarz DE, O'Connell LA, et al. Protection from UV light is an evolutionarily conserved feature of the haematopoietic niche. *Nature* 2018;558:445-8. doi: 10.1038/s41586-018-0213-0.
41. Matsuoka S, Ebihara Y, Xu M, Ishii T, Sugiyama D, Yoshino H, et al. CD34 expression on long-term repopulating hematopoietic stem cells changes during developmental stages. *Blood* 2001;97:419-25.
42. Armin A. Changes in the cell surface markers during normal hematopoiesis: A guide to cell isolation. *G J Hematol Blood Trans* 2014;1:20-8.
43. Scapigliati G, Mazzini M, Mastrolia L, Romano N, Abelli L. Production and characterization of a monoclonal antibody against the thymocytes of the sea bass *Dicentrarchus labrax* (L.) (Teleostea, Percichthyidae). *Fish Shellfish Immun* 1995;5:393-405.
44. Scapigliati G, Romano N, Picchietti S, Mazzini M, Mastrolia L, Scalia D, et al. Monoclonal antibodies against sea bass *Dicentrarchus labrax* (L) immunoglobulins: immunolocalization of immunoglobulin-bearing cells and applicability in immunoassays. *Fish Shellfish Immun* 1996;6:383-401.
45. Scapigliati G, Romano N, Abelli L. Monoclonal antibodies in teleost fish immunology: identification, ontogeny and activity of T- and B-lymphocytes. *Aquaculture* 1999;172:3-28.
46. Romano N, Rossi F, Abelli L, Caccia E, Piergentili R, Mastrolia L, et al. Majority of TcRbeta+ T-lymphocytes located in thymus and midgut of the bony fish, *Dicentrarchus labrax* (L.). *Cell Tissue Res* 2007;329:479-89.
47. Lauriano ER, Pergolizzi S, Aragona M, Montalbano G, Guerrera MC, Crupi R, et al. Intestinal immunity of dogfish *Scyliorhinus canicula* spiral valve: A histochemical, immunohistochemical and confocal study. *Fish Shellfish Immun* 2019;87:490-8. doi: 10.1016/j.fsi.2019.01.049.
48. Moczek AP, Sears KE, Stollewerk A, Wittkopp PJ, Diggle P, Dworkin I, et al. The significance and scope of evolutionary developmental biology: a vision for the 21st century. *Evol Dev* 2015;17:198-219. doi: 10.1111/ede.12125.